

1 **A critical role for hepatic protein arginine methyltransferase 1 isoform 2 in glycemic control.**

2

3 **Running title: Hepatic PRMT1 in glycemic control**

4

5 Yingxu Ma^{1,3}, Shanshan Liu¹, Heejin Jun¹, Jine Wang¹, Xiaoli Fan⁵, Guobing Li¹, Lei Yin²,
6 Liangyou Rui², Steven A. Weinman⁴, Jianke Gong^{1,5}, Jun Wu^{1,2}

7

8 ¹Life Sciences Institute, University of Michigan, Ann Arbor, Michigan 48109, USA.

9 ²Department of Molecular & Integrative Physiology, University of Michigan Medical School, Ann
10 Arbor, Michigan 48109, USA.

11 ³Department of cardiology, The Second Xiangya Hospital, Central South University, Changsha,
12 Hunan 410013, China.

13 ⁴Department of Internal Medicine and the Liver Center, University of Kansas Medical Center,
14 Kansas City, Kansas 66160, USA.

15 ⁵International Research Center for Sensory Biology and Technology of MOST, Key Laboratory
16 of Molecular Biophysics of MOE, and College of Life Science and Technology, and Huazhong
17 University of Science and Technology, Wuhan, Hubei, 430074, China.

18 Correspondence: College of Life Science and Technology, Key Laboratory of Molecular
19 Biophysics of MOE, Huazhong University of Science and Technology, Wuhan, Hubei, 430074,
20 China. E-mail: jiankeg@umich.edu (J. Gong). Life Sciences Institute, University of Michigan,
21 Ann Arbor, MI, 48109, USA. E-mail: wujunz@umich.edu (J. Wu).

22

23

24

This is the author manuscript accepted for publication and has undergone full peer review but has not been through the copyediting, typesetting, pagination and proofreading process, which may lead to differences between this version and the [Version of Record](#). Please cite this article as [doi: 10.1002/FSB2.21018](https://doi.org/10.1002/FSB2.21018)

This article is protected by copyright. All rights reserved

25

26 Abbreviations:

cAMP	Cyclic adenosine monophosphate
CHX	Cycloheximide
CRM1	Chromosome region maintenance 1/exportin1/Exp1/Xpo1
GAN	Gubra Amylin NASH
GTT	Glucose tolerance test
HFD	High fat diet
NASH	Nonalcoholic steatohepatitis
PRMT	Protein arginine methyltransferase
PTT	Pyruvate tolerance test
STZ	Streptozocin

27

28 **Abstract**

29 Appropriate control of hepatic gluconeogenesis is essential for the organismal survival upon
30 prolonged fasting and maintaining systemic homeostasis under metabolic stress. Here we show
31 protein arginine methyltransferase 1 (PRMT1), a key enzyme that catalyzes the protein arginine
32 methylation process, particularly the isoform encoded by *Prmt1* variant 2 (*PRMT1V2*), is critical
33 in regulating gluconeogenesis in the liver. Liver-specific deletion of *Prmt1* reduced gluconeogenic
34 capacity in cultured hepatocytes and in the liver. *Prmt1v2* was expressed at a higher level compared
35 to *Prmt1v1* in hepatic tissue and cells. Gain-of-function of PRMT1V2 clearly activated the
36 gluconeogenic program in hepatocytes via interactions with PGC1 α , a key transcriptional
37 coactivator regulating gluconeogenesis, enhancing its activity via arginine methylation, while no
38 effects of PRMT1V1 were observed. Similar stimulatory effects of PRMT1V2 in controlling
39 gluconeogenesis were observed in human HepG2 cells. PRMT1, specifically PRMT1V2, was
40 stabilized in fasted liver and hepatocytes treated with glucagon, in a PGC1 α -dependent manner.
41 PRMT1, particularly *Prmt1v2*, was significantly induced in the liver of streptozocin-induced type
42 1 diabetes and high fat diet-induced type 2 diabetes mouse models and liver-specific *Prmt1*
43 deficiency drastically ameliorated diabetic hyperglycemia. These findings reveal that PRMT1
44 modulates gluconeogenesis and mediates glucose homeostasis under physiological and

45 pathological conditions, suggesting that deeper understanding how PRMT1 contributes to the
46 coordinated efforts in glycemic control may ultimately present novel therapeutic strategies that
47 counteracts hyperglycemia in disease settings.

48

49 **Keywords:** PRMT1 variant 2; Glycemic control; Liver function; Diabetic hyperglycemia

50

51 **Introduction**

52 Glucose homeostasis is of great importance for survival and metabolic health in general.
53 Blood glucose levels must be maintained within a narrow range to avoid hypoglycemia during
54 periods of fasting and hyperglycemia after calorie overload. Liver plays a key role in the regulation
55 of systemic glucose levels because hepatic glucose production contributes to 80% of total
56 endogenous glucose production (1). Hepatic glycogenolysis is mainly responsible for glucose
57 production in the short-term fasting but gluconeogenesis is of much greater importance during
58 prolonged fasting (2). Hepatic gluconeogenesis is mainly controlled by the availability of
59 substrates and the rate-limiting enzymes phosphoenolpyruvate carboxykinase 1 (encoded by *Pck1*)
60 and glucose-6-phosphatase (encoded by *G6pc*). This process is tightly modulated through the
61 actions of insulin and glucagon, which coordinately respond to nutrient status. In patients with
62 diabetes and other metabolic disorders, inappropriate activation of gluconeogenesis and
63 development of insulin resistance renders hyperglycemia.

64 Peroxisome proliferative activated receptor- γ co-activator 1 (PGC1 α) was originally
65 identified in brown fat, regulating adaptive thermogenesis as a transcriptional coactivator (3).
66 Further investigation revealed that PGC1 α can be induced by cyclic adenosine monophosphate
67 (cAMP) in primary hepatocytes and was significantly induced in the liver by fasting (4). PGC1 α
68 is the master modulator of hepatic metabolism through regulation of gluconeogenesis, lipid
69 catabolism, mitochondrial biogenesis via interactions with many key factors, including forkhead
70 transcription factor (FOXO1), hepatocyte nuclear factor 4 α (HNF4 α) and Sirtuin 1 (SIRT1) (4-7).
71 The activity of PGC1 α is closely monitored and tightly controlled at transcriptional and
72 posttranslational levels to accommodate its versatile functions in various physiological processes
73 (8), including arginine methylation (9).

74 Methylation of arginine residues is a common post-translational modification and is regulated
75 by a family of gene products called protein arginine methyltransferases (PRMTs) (10). PRMTs are
76 classified as type I (PRMT1, 2, 3, 4, 6, and 8), type II (PRMT5 and 9) and type III (PRMT7) on
77 the basis of their methylation manner (11). PRMT1 is the predominant member of the PRMT
78 family, contributing to around 85% of protein arginine methylation in mammalian cells and tissues.
79 It has been reported that PRMT1 modulates insulin signaling (12), maintains cardiac function (13),
80 mediates lipogenesis in the liver (14), and regulates thermogenesis in fat (15). *Prmt1* has different
81 splicing variants with distinct subcellular localization, substrate specificity, and enzyme activity
82 (16). Among all these isoforms, *PRMT1V1* and *PRMT1V2* are the two main variants in normal
83 human tissues (16). The difference between these two isoforms is that *PRMT1V1* has a
84 chromosome maintenance 1/exportin1/Exp1/Xpo1 (CRM1)-dependent nuclear export
85 sequence which is coded by exon 2 (15, 16).

86 In this study, multiple lines of in vitro and in vivo evidence generated from gain- and loss-of-
87 function models strongly support the hypothesis that PRMT1, variant 2 in particular, plays an
88 essential role in regulating hepatic gluconeogenesis via interactions with PGC1 α . PRMT1V2 was
89 induced in the liver of mouse models mimicking diabetes and other metabolic disorders where
90 pathological hyperglycemia was observed. Mice with hepatocyte-specific *Prmt1* deletion
91 displayed less elevated blood glucose levels and improved glucose homeostasis when challenged
92 with streptozocin or high fat diet (HFD), indicating inhibition of hepatic PRMT1 activity may
93 represent therapeutic opportunities counteracting inappropriate gluconeogenesis in human
94 diseases.

95

96

97

98

99

100

101

102

103

104

105

106

107 **Materials and Methods**

108 **Reagents**

109 Glucagon (G2044), forskolin (F6886), insulin (I5500, for in vitro studies), dexamethasone
110 (D4902), fetal bovine serum (FBS) (F0926), cycloheximide (CHX; C4859), MG132 (M7449),
111 ammonium chloride (NH₄Cl; A9434), and streptozocin (STZ; S0130) were purchased from Sigma-
112 Aldrich. Insulin (NDC 0002-8215-01, for in vivo studies) was purchased from Eli Lilly. Hanks'
113 Balanced Salt Solutions (HBSS; SH3058802) was purchased from Thermo Fisher Scientific.
114 Dulbecco's Modified Eagle Medium/Nutrient Mixture F-12 GlutaMAX (DMEM/F12 GlutaMAX)
115 (10565-042), DMEM (11995073), DMEM-low glucose (11885084), and penicillin streptomycin
116 solution (15140122) were purchased from Life Technologies. Collagenase Type IV (LS004188)
117 was purchased from Worthington Biochemical. Polyethylenimine (PEI; linear, molecular mass of
118 25 kDa; 23966-1) was purchased from Polysciences, Inc.

119 **Animal studies**

120 All the mouse studies were conducted according to the protocol reviewed and approved by
121 the Institutional Animal Care and Use Committee at the University of Michigan. All mice were
122 housed under 12-hour light/12-hour dark cycle with an *ad libitum* chow diet (5L0D; PicoLab
123 Laboratory Rodent Diet) unless otherwise indicated. The C57BL/6J (000664) and *Albumin-Cre*
124 (003574) mice were obtained from the Jackson Laboratory. *Prmt1*^{fl/fl} mice were obtained from Dr.
125 Steven A. Weinman. The conditioned alleles lead to Cre-mediated deletion of exon 4 and 5 of
126 *Prmt1* gene (17). Liver-specific *Prmt1* KO mice (*Alb-Cre;Prmt1*^{fl/fl}) were generated by crossing
127 *Prmt1*^{fl/fl} and *Alb-Cre* mice. For the fasting experiments, mice were fasted during the dark period
128 for indicated time. Blood glucose levels were measured in tail blood by using the OneTouch Ultra
129 Glucometer (Lifescan). For adenovirus infusion studies, indicated adenoviruses were injected into

130 anesthetized mice through tail vein. For STZ studies, mice were intraperitoneally injected with
131 either vehicle or 100 mg per kg body weight per day STZ for one week. For HFD-induced obesity
132 study, mice were singly housed on either a chow diet or a HFD that consists of 45% of calories
133 from fat (D12451, Research Diets) for indicated time. Over this period, body weights and food
134 intake were measured weekly. For diet-induced nonalcoholic steatohepatitis (NASH) study, mice
135 were singly housed on either a chow diet or Gubra Amylin NASH (GAN) diet (D09100310,
136 Research Diets). Over this period, body weights and food intake were measured weekly. Both male
137 and female were used in this study and similar results were observed in both genders.

138 **Quantitative real-time PCR**

139 Total RNA was extracted from cells and tissues using TRI reagent (T9424, Sigma-Aldrich)
140 according to the manufacturer's instructions. cDNA was synthesized using M-MLV Reverse
141 Transcriptase (28025021, Life Technologies). Quantitative real-time PCR (qPCR) reactions were
142 performed with SYBR Green (4368708, Thermo Fisher Scientific) on a QuantStudio 5 Real Time
143 PCR system (Thermo Fisher Scientific). Results were analyzed by using the $2^{-\Delta\Delta C_t}$ method and
144 normalized to levels of TATA-box binding protein (*Tbp*). All qPCR primer sequences are listed in
145 Supplementary Table.

146 **Western blot**

147 Total protein from cells and liver tissue was extracted in ice-cold radioimmunoprecipitation
148 assay buffer (RIPA buffer) (150 mM NaCl, 50 mM Tris-HCl pH 8.0, 5 mM EDTA, 0.5% sodium
149 deoxycholate, 0.1% SDS, 1% NP-40) supplemented with protease inhibitor cocktail (Sigma-
150 Aldrich). Protein concentration was measured by DC protein assay reagents (Bio-Rad Laboratories)
151 in SpectraMax M3 multi-mode microplate reader (Molecular Devices). Protein lysate was
152 subjected to SDS-PAGE and transferred to polyvinylidene fluoride (PVDF) membranes. After
153 incubation with blocking buffer (5% nonfat milk in 1% TBS with Tween 20) for 1 hour, the
154 membranes were probed with primary anti-PRMT1 (Cell Signaling Technology, catalog 2449S),
155 anti-HSP90 (Cell Signaling Technology, catalog 4874S), anti-HA (Cell Signaling Technology,
156 catalog 3724), anti- α -tubulin (Cell Signaling Technology, catalog 2144), anti-Adme-R (Cell
157 Signaling Technology, catalog 13522), anti-pAkt (Cell Signaling Technology, catalog 9271S),
158 anti-Akt (Cell Signaling Technology, catalog 9272), and anti-Histone H3 (Active motif, catalog
159 39763). Secondary antibody linked with horseradish peroxidase was diluted in 5% nonfat milk in

160 1% TBS with Tween 20 and incubated for 2 hours at room temperature. The blots were developed
161 by ECL (Bio-Rad Laboratories, 1705061). Quantification of immunoblot analyses was performed
162 using Quantity One (Bio-Rad).

163 **Subcellular fractionation**

164 Liver tissue was minced in ice-cold cytoplasm extraction buffer (20 mM HEPES, 1 mM
165 EDTA, 10 mM NaCl, 2 mM MgCl₂, 0.25% NP-40) supplemented with protease inhibitor cocktail
166 (Sigma-Aldrich) whereas cells were scraped in ice-cold cytoplasm extraction buffer. The
167 homogenate was vortexed for 15 seconds followed by 5 minute incubation at 4°C for 6 times. The
168 lysate was centrifuged at 5000g at 4°C for 5 minutes to get the supernatant containing cytoplasmic
169 fraction. The pellet after centrifugation was vortexed for 15 seconds and incubated at 4°C for 10
170 minutes in ice-cold nuclear extraction buffer (20 mM HEPES, 1 mM EDTA, 420 mM NaCl, 2 mM
171 MgCl₂, 0.25% NP-40, 25% glycerol) supplemented with protease inhibitor cocktail (Sigma-
172 Aldrich). The homogenate was centrifuged at 14,000g at 4°C for 5 minutes to get the supernatant
173 containing nuclear fraction.

174 **Immunoprecipitation**

175 Hepa 1-6 cells were infected with indicated adenoviruses or transiently transfected with
176 indicated plasmids. At 48 hours following infection or transfection, cells were lysed with ice-cold
177 RIPA buffer on a shaker at 4°C for 1 hour. The lysate was centrifuged at 14,000g for 15 minutes
178 at 4°C to pellet debris and the supernatant was transferred into a fresh Eppendorf tube. After
179 quantification by DC assay, 1 mg of protein for each group was incubated with anti-PGC1 α
180 (Millipore, catalog ST1202) overnight at 4°C with rotation. Five percent of the lysate was saved
181 as input. Thirty microliters of protein G-agarose (Santa Cruz Biotechnology, catalog sc-2002) was
182 washed with RIPA buffer 3 times and then added into protein lysate following rotation at 4°C for
183 3 hours. The beads were pelleted by quick spin and washed with RIPA buffer 3 times. After
184 removing supernatant, 30 μ L of sample buffer was added to elute the immunoprecipitated proteins
185 followed by boiling at 98°C for 5 minutes. The immunoprecipitated protein was subjected to
186 immunoblotting as described above.

187 **Tolerance tests**

188 For pyruvate tolerance test (PTT), mice were fasted for 16 hours and then intraperitoneally
189 injected with sodium pyruvate (1.75 g/kg). For glucose tolerance test (GTT), mice were fasted for
190 16 hours and then intraperitoneally injected with glucose (1 g/kg). The blood glucose levels were
191 measured in tail blood at indicated time points by using the OneTouch Ultra Glucometer (Lifescan).

192 **Cell culture**

193 Mouse primary hepatocytes were isolated and cultured as previously reported (15). In brief,
194 the liver was perfused with washing buffer (HBSS buffer supplemented with 0.5 mM EGTA pH
195 7.4 and 25 mM HEPES pH 7.4) and then with digestion medium (DMEM-low glucose
196 supplemented with 1% penicillin-streptomycin, 15 mM HEPES pH 7.4, and 100 U/mL collagenase
197 IV) via the inferior vena cava after the anesthesia of the mouse. After dispersing the cells, they
198 were filtered by using a prechilled BD disposable falcon tube nylon filter. Hepatocytes were
199 washed twice by using isolation medium (DMEM/F12 GlutaMAX supplemented with 10% FBS,
200 1% penicillin-streptomycin, 1 μ M dexamethasone and 0.1 μ M insulin) and seeded on collagen
201 coated 12-well plates at 3×10^5 cells/mL with the isolation medium. One hour after plating, the
202 medium was changed to culture medium (DMEM-low glucose supplemented with 10% FBS, 1%
203 penicillin-streptomycin, 0.1 μ M dexamethasone, and 1 nM insulin). Cells will be serum starved
204 for 24 hours before treatments (such as glucagon).

205 Hepa 1-6 cells and HepG2 cells were obtained from ATCC and maintained in DMEM
206 supplemented with 10% FBS and 1% penicillin-streptomycin. Particularly, HepG2 cells were
207 seeded on culture plates coated with type I rat tail collagen (CB354249, Fisher Scientific).

208 **Histology**

209 Liver tissues were fixed in 10% formalin at 4°C overnight. Paraffin embedding and
210 hematoxylin and eosin (H&E) staining were performed by the University of Michigan
211 Comprehensive Cancer Center Research Histology and Immunoperoxidase Laboratory. Images
212 were obtained by using LEICA DM2000.

213 **Adenovirus production**

214 Adenoviruses that overexpress GFP, CRE, PGC1 α (18), HA-PRMT1V1, and HA-PRMT1V2
215 (15) were generated as previously described. Adenoviruses expressing shRNA against *Ppgargc1a*

216 (6) and *PRMT1* (15) were produced as previously described. Media were refreshed 16-24 hours after
217 infection and high efficiency of virus transduction that exceeded 90% was verified by the number
218 of GFP-positive cells under fluorescence microscope.

219 **Luciferase reporter assays**

220 Plasmids expressing PRMT1V1, PRMT1V2 (15), PRMT1V2-G98R (19, 20), FOXO1 (21),
221 PGC1 α (18), PGC1 α - Δ E, PGC1 α -R3K (9) and the *Pck1* promoter luciferase reporter (4) were
222 described previously. Hepa 1-6 cells or HepG2 cells were seeded into 12-well plates and
223 transiently transfected with plasmids expressing PGC1 α (909 ng), PGC1 α - Δ E (909 ng), PGC1 α -
224 R3K (909 ng), or FOXO1 (909 ng) and/or PRMT1V1 (909 ng), PRMT1V2 (909 ng) or
225 PRMT1V2-G98R (909 ng) by using PEI method together with *Pck1* promoter luciferase reporter
226 construct (90.0 ng) and *Renilla* luciferase reporter construct (10 ng) unless otherwise specified.
227 Cells were lysed 48 hours after transfection. Luciferase activity was measured by a luciferase assay
228 kit (PR-E1941, Promega) according to the manufacturer's recommendations by using a Perkin
229 Elmer Enspire Model 2300 Multilabel Microplate Reader (PerkinElmer). Firefly luciferase activity
230 was normalized to *Renilla* luciferase activity.

231 **Statistics**

232 Data are presented as mean \pm SEM. Two-tailed unpaired Student's *t* test was used for
233 comparison of two genotypes or treatments. One-way ANOVA or 2-way ANOVA was performed
234 to compare 3 or more groups, as indicated in the figure legends. All the statistical analyses were
235 performed using SPSS (IBM).

236

237

238

239

240

241

242

243

244

245

246 **Results**

247 **Hepatic *Prmt1* deficiency renders impaired gluconeogenesis in the liver**

248 To investigate the role of PRMT1 in regulating hepatic glucose metabolism, we first
249 examined wild-type (WT) mice subjected to fasting for 16 hours. As expected, mice in the fasted
250 state had lower body weights and reduced blood glucose levels compared to mice with free access
251 to food (Figure 1A). qPCR analyses revealed that expression levels of key gluconeogenic genes,
252 including *Pck1*, *G6pc*, *Ppargc1a*, and CCAAT/enhancer binding protein beta (*Cebpb*), were
253 elevated in the liver isolated from mice after overnight fasting compared to those of fed controls
254 (Figure 1A). It is of great interest that fasting significantly increased global asymmetric arginine
255 dimethylation with increased PRMT1 expression on the protein level but not transcriptionally in
256 the liver (Figure 1, A and B). To mechanistically investigate the posttranscriptional induction of
257 PRMT1 expression in the liver in the fasting state, a cycloheximide chase experiment was
258 performed to reveal whether this is due to changes in the rate of protein degradation. Treatment
259 with gluconeogenic stimulating hormone, glucagon, dramatically extended the half-life of PRMT1
260 from 1.6 hours to 3 hours when primary hepatocytes from WT mice were treated with
261 cycloheximide, a commonly used protein synthesis inhibitor (22) (Figure 1C). Further
262 investigation revealed that increased PRMT1 protein accumulation was observed in the primary
263 hepatocytes treated with a proteasome inhibitor MG132 (22) but not NH₄Cl, a lysosome inhibitor
264 (23), suggesting that proteasomal pathways may be involved (Supplementary Figure 1, A and B).

265 In addition to being stimulated by glucagon after prolonged fasting, gluconeogenesis is also
266 governed by the suppressive effects of insulin postprandially. Reduced suppression of hepatic
267 glucose production rendered by insulin resistance is one of key causes for hyperglycemia observed
268 in type 2 diabetes (24). Therefore, we next investigated whether insulin is also involved in the
269 regulation of hepatic PRMT1. WT mice were subjected to fasting for 16 hours, followed by
270 intraperitoneal injection with insulin. Insulin treatment did not lead to changes in PRMT1 mRNA
271 or protein levels (Supplementary Figure 1, C and D). Similarly, no changes were observed in

272 PRMT1 mRNA and protein in vitro in primary hepatocytes treated with insulin (Supplementary
273 Figure 1, E and F), indicating minimal regulatory effects through insulin in this context.

274 To determine whether *Prmt1* is required in the hepatic gluconeogenesis, we generated liver-
275 specific *Prmt1* KO mice (*Alb-Cre;Prmt1^{fl/fl}*) by crossing *Prmt1^{fl/fl}* mice with *Albumin-Cre* mice.
276 Hepatocyte-specific deletion of *Prmt1* did not cause any gross abnormality under the basal
277 conditions. *Alb-Cre;Prmt1^{fl/fl}* mice showed no differences in body weight and morphological
278 architecture in the liver compared with *Prmt1^{fl/fl}* controls (Figure 1, D and E). *Prmt1* deletion was
279 confirmed by qPCR in the liver and no deletion was detected in other tissues that express *Prmt1*
280 (Figure 1F). Additionally, no other *Prmts* were induced to compensate for the loss of *Prmt1*
281 expression in the liver (Supplementary Figure 2A). Western blot analyses further confirmed
282 PRMT1 deletion in the liver with significantly reduced global asymmetric arginine dimethylation
283 (Figure 1G), consistent with the notion that PRMT1 plays a predominant role in the liver among
284 all the PRMTs (25). *Alb-Cre;Prmt1^{fl/fl}* mice exhibited no changes in gluconeogenic gene
285 expression in the liver under the fed state (Figure 1H). It has previously been reported that deletion
286 of *Prmt1* in the liver may influence cellular response to stresses rendered by environmental insults
287 such as alcohol (26). Decreased expression of oxidative stress response genes (*Sod1* and *Sod2*),
288 increased expression of proliferation markers (*Cyclin B1* and *c-Myc*) and comparable expression
289 of genes regulating inflammation, cell death and fibrosis were observed in the liver of *Alb-*
290 *Cre;Prmt1^{fl/fl}* mice compared to that in the *Prmt1^{fl/fl}* controls under basal conditions (ad lib)
291 (Supplementary Figure 2B), consistent with previous observations (26). After overnight fasting,
292 *Alb-Cre;Prmt1^{fl/fl}* mice had lower blood glucose levels and decreased expression of gluconeogenic
293 genes compared to littermate control mice (Figure 1, I and J). Yet, fasting did not result in changes
294 in the expression pattern of the stress response genes between the two genotypes (Supplementary
295 Figure 2C), suggesting the blunted gluconeogenesis in the *Prmt1*-deleted liver after fasting was
296 mediated through a specific regulatory signaling pathway rather than due to global defects or organ
297 failure. PTT revealed that hepatic gluconeogenesis was impaired after the deletion of *Prmt1*
298 (Figure 1K). It has been reported that global haploinsufficiency of *Prmt1* resulted in impaired
299 gluconeogenesis and significant reduction of PRMT1 protein levels in the liver (27). However, no
300 differences in the expression of gluconeogenic genes were observed in the liver of *Alb-*
301 *Cre;Prmt1^{fl/+}* mice compared to those of *Prmt1^{fl/fl}* mice after overnight fasting. Furthermore,
302 western blot analyses revealed that PRMT1 protein levels were comparable in the liver from *Alb-*

303 *Cre;Prmt1^{fl/+}* mice to those of littermate *Prmt1^{fl/fl}* mice controls (Supplementary Figure 2, D and
304 E).

305 Similar to what was observed in the *Alb-Cre;Prmt1^{fl/fl}* mice where *Prmt1* was deleted
306 developmentally, acute hepatic deletion of *Prmt1* mediated by adenoviral expression of
307 recombinase Cre led to lower fasting blood glucose, less induced hepatic gluconeogenic gene
308 expression after fasting and less glucose production upon pyruvate challenges with no gross
309 differences and morphological changes in the liver under ad lib conditions (Supplementary Figure
310 3, A-H, and data not shown). The cell-autonomous regulation of hepatic gluconeogenesis through
311 PRMT1 was further confirmed by the observation that *Prmt1* deletion significantly blunted the
312 glucagon-mediated induction of *Pck1*, *G6pc*, *Ppargc1a*, and *Cebpb* in the primary hepatocytes
313 (Supplementary Figure 3, I and J).

314 We next investigated whether the effects of PRMT1 on gluconeogenesis are conserved in
315 human using a loss-of-function model (Figure 1L). Treatment of glucagon plus forskolin
316 (increasing intracellular cAMP levels) activated the gluconeogenic program in HepG2 cells, a
317 commonly used human hepatoma cell line (Figure 1M), in agreement with previous results (28).
318 However, knockdown of *PRMT1* significantly ablated the response of HepG2 cells to glucagon
319 plus forskolin stimulation (Figure 1M), confirming that the role of PRMT1 in glucose regulation
320 is conserved in human liver cells.

321 **PRMT1V2 plays a dominant role in activating the hepatic gluconeogenic program**

322 Among the various isoforms of PRMT1, which one(s) may contribute primarily to this critical
323 role in gluconeogenic regulation is completely unknown. We first investigated the relative
324 expression of *Prmt1v1* and *Prmt1v2* in the liver, the two dominant isoforms in humans that differs
325 from each other by a CRM1-dependent nuclear export sequence (Figure 2A) (16). We found that
326 the expression of *Prmt1v2* was higher than *Prmt1v1* in the liver from WT mice (Supplementary
327 Figure 4A). A similar expression pattern of *Prmt1v1* and *Prmt1v2* was observed in primary
328 hepatocytes isolated from WT mice, Hepa 1-6 cells (a murine hepatoma cell line) and HepG2 cells
329 (Supplementary Figure 4, B-D). Interestingly, western blot analyses of subcellular fractionations
330 revealed that PRMT1 expression within the nucleus was increased in the fasted liver while
331 cytosolic PRMT1 remained unchanged (Figure 2B), suggesting that PRMT1V2 might be the
332 isoform that activates hepatic gluconeogenesis.

333 To further explore the role of these two isoforms in the hepatic glucose production, gain-of-
334 function experiments were carried out with adenoviruses that overexpress PRMT1V1 and
335 PRMT1V2, which displayed subcellular expression pattern as expected (Figure 2, C-G,
336 Supplementary Figure 4, E-G). Overexpression of PRMT1V2 significantly induced the expression
337 of gluconeogenic genes in the mouse primary hepatocytes whereas little effects were observed in
338 cells overexpressing PRMT1V1 (Figure 2, D and F).

339 To test this effect in vivo, we ectopically expressed PRMT1V1 and PRMT1V2 in the mice
340 with hepatic deletion of endogenous *Prmt1* (Figure 2, H-J). Mice injected with adenovirus
341 overexpressing PRMT1V2 displayed higher blood glucose levels after fasting for 6 and 16 hours
342 (Figure 2K). However, there was no difference in fasted blood glucose levels between mice
343 injected with adenovirus overexpressing GFP and PRMT1V1 (Figure 2K). In addition,
344 gluconeogenic genes, including *Pck1*, *G6pc*, *Ppargc1a*, and *Cebpb*, were significantly induced in
345 mice with PRMT1V2 overexpression, but not PRMT1V1, after 16-hour fasting (Figure 2L). PTT
346 results demonstrated that hepatic gluconeogenic capacity was augmented in mice with PRMT1V2
347 overexpression but remained unchanged in mice with PRMT1V1 overexpression (Figure 2M).
348 Similar to what was observed in murine primary hepatocytes, overexpression of PRMT1V1 did
349 not affect the gluconeogenic program in HepG2 cells (Figure 2, N and O). On the contrary,
350 PRMT1V2 overexpression significantly increased the expression of gluconeogenic genes (Figure
351 2, P and Q). These results suggest that PRMT1V2 plays a major role in regulating hepatic
352 gluconeogenesis.

353 **PRMT1V2 stimulates hepatic gluconeogenesis via PGC1 α**

354 PGC1 α is a transcriptional coactivator that regulates multiple physiological functions in
355 metabolism, including adaptive thermogenesis and gluconeogenesis (3, 4, 29). It has been reported
356 that the arginine residues of PGC1 α could be methylated by PRMT1 and its coactivator activity
357 was increased after methylation (9). Consistent with previous reports (4), overexpression of
358 PGC1 α significantly induced the expression of gluconeogenic genes (Figure 3A). Co-
359 overexpression of PRMT1V2 but not PRMT1V1 with PGC1 α can lead to further increase in
360 expression levels of gluconeogenic genes in primary hepatocytes, likely through activated PGC1 α
361 that was methylated primarily by nucleus-located PRMT1V2 but not PRMT1V1 in the cytosol
362 (Figure 3, B and C). This gluconeogenic effect of PRMT1V2 was also observed in experiments

363 testing *Pck1* promoter activity in Hepa 1-6 cells (Figure 3, D and E). In Hepa 1-6 cells, knockdown
364 of *Ppargc1a* reduced *Pck1*-luciferase activity (Figure 3, F-H). Transient transfection of PRMT1V2
365 increased *Pck1*-luciferase activity while there were no effects observed in cells transfected with
366 PRMT1V1 (Figure 3, G and H). Notably, knockdown of *Ppargc1a* completely abolished the
367 stimulatory effects of PRMT1V2 (Figure 3H). This drastic effects of PGC1 α on PRMT1V2
368 function in the hepatic gluconeogenic regulation were further revealed when PRMT1V1 and
369 PRMT1V2 were individually re-introduced back in *Alb-Cre;Prmt1^{fl/fl}* mice after knockdown of
370 *Ppargc1a* (Figure 3, I-K). Elevated fasting blood glucose levels, induced gluconeogenic gene
371 expression and compromised pyruvate tolerance observed previously with PRMT1V2
372 overexpression were completely blunted in the absence of PGC1 α (Figure 3, I-K). Similar results
373 were observed in vitro in the primary hepatocytes demonstrating a likely cell-autonomous
374 mechanism (Supplementary Figure 5, A and B). Conversely, even though injection with the
375 adenovirus encoding an shRNA specific to *Ppargc1a* decreased the gluconeogenic capacity as
376 expected in the *Prmt1^{fl/fl}* mice, knockdown of *Ppargc1a* did not render further reduction in
377 gluconeogenesis in *Alb-Cre;Prmt1^{fl/fl}* mice, demonstrating the physiological significance of this
378 PGC1 α and PRMT1 interaction in vivo. (Supplementary Figure 5, C-E).

379 It has been reported that PRMT1 may regulate glucose production through FOXO1, a
380 transcription factor known to activate gluconeogenesis in the liver (27, 30). But which isoform of
381 PRMT1 may be involved in this process has not been investigated. In contrast to the dominant
382 effects of PRMT1V2 when working with PGC1 α , both PRMT1V1 and PRMT1V2 can further
383 increase *Pck1*-luciferase activity when co-overexpressed with FOXO1 (Supplementary Figure 6,
384 A and B). This coactivation between PRMT1 and FOXO1 remained functional in the cells infected
385 with an adenovirus encoding an shRNA specific to *Ppargc1a* (Supplementary Figure 6, C and D),
386 suggesting that PRMT1 may regulate hepatic gluconeogenesis with different partners through
387 various mechanisms.

388 We next explored whether PRMT1V2 functions with PGC1 α in hepatic gluconeogenic
389 regulation in human liver cells. Similar to what we observed in murine hepatocytes, co-
390 overexpression of PRMT1V2 and PGC1 α further increased gluconeogenic gene expression and
391 *Pck1* promoter activity compared with those observed in cells only ectopically overexpressing
392 PGC1 α , whereas little effects were observed with PRMT1V1 (Figure 3, L-O).

393 Further mechanistic investigation was carried out to test whether PRMT1V2 enhances
394 PGC1 α activity through arginine methylation. In contrast to what was observed with the wild-type
395 PRMT1V2, which increased *Pck1*-luciferase activity when co-overexpressed with PGC1 α ,
396 PRMT1V2-G98R, a catalytically inactive mutant (Figure 4, A and B) (19, 20), did not show any
397 synergistic effects with PGC1 α mediating *Pck1* promoter activation (Figure 4C). It has been
398 proposed that the potential methylation sites of PRMT1 on PGC1 α , arginine residues 665, 667,
399 and 669, locate within the C-terminal E region (9). Even though when expressed alone, either a
400 mutant PGC1 α - Δ E without E region or a mutant PGC1 α -R3K consisting of conversion of arginine
401 residues 665, 667, and 669 to lysine can increase *Pck1*-luciferase activity, neither mutant
402 demonstrated coactivation effects when co-expressed with PRMT1V2 (Figure 4, D-H). These
403 results collectively support the hypothesis that PRMT1V2 mediates PGC1 α function primarily
404 through arginine methylation.

405 Our results demonstrated that PRMT1, variant 2 in particular, modulated hepatic
406 gluconeogenesis via PGC1 α . We next tested, as the master regulator of gluconeogenesis, whether
407 PGC1 α regulates PRMT1 expression in hepatocytes. PGC1 α overexpression in HepG2 cells did
408 not lead to changes in *PRMT1* mRNA levels (Figure 4I), whereas increased protein levels of
409 PRMT1 were detected in cells with adenovirus overexpressing PGC1 α (Figure 4J). It has been
410 reported that PRMT1 protein can be stabilized through downregulation of p300 (EP300) and
411 Sirtuin 1 (Sirt1) (22). Indeed, overexpression of PGC1 α led to decreased expression of *EP300* and
412 *SIRT1* in HepG2 cells (Figure 4K). Furthermore, glucagon treatments no longer stabilized PRMT1
413 in the hepatocytes in the absence of PGC1 α (Figure 4L). These results collectively suggest that as
414 a part of the machinery of glucose control in the liver, PRMT1 itself is regulated by PGC1 α , which
415 forms a feedback regulatory loop.

416 **Liver-specific *Prmt1* deficiency counteracts diabetic hyperglycemia**

417 Excessive hepatic gluconeogenesis and loss of glycemic control is one of the characteristics
418 of diabetes and metabolic syndrome (1, 31, 32). Whether PRMT1 modulates pathological hepatic
419 glucose production in diabetes may be of great clinical relevance. Streptozocin (STZ) is widely
420 used to kill insulin-producing beta cells, causes acute glucotoxicity effects in vivo and induces
421 type 1 diabetes in mice (33). Mice injected with STZ displayed higher fed blood glucose levels
422 when compared with mice injected with vehicle (Figure 5A). In this type 1 diabetes mouse model,

423 *Prmt1* was markedly increased along with the induction of gluconeogenic genes (Figure 5, A and
424 B). It is of note that *Prmt1v1* was not changed but *Prmt1v2* was significantly induced in the liver
425 of mice injected with STZ (Figure 5A). These results suggest that PRMT1 is involved in the
426 inappropriate hepatic glucose production in diabetes.

427 To investigate how the absence of *Prmt1* may affect pathological hepatic gluconeogenesis,
428 we injected *Alb-Cre;Prmt1^{fl/fl}* and *Prmt1^{fl/fl}* control mice with STZ. After STZ injection, liver-
429 specific deletion of *Prmt1* resulted in less elevated blood glucose levels and less induced
430 gluconeogenic gene expression in the liver in the fed state compared to STZ-injected *Prmt1^{fl/fl}*
431 control mice (Figure 5, C and D). GTT revealed that *Alb-Cre;Prmt1^{fl/fl}* mice had better control of
432 glycemia after STZ injection (Figure 5E). These results indicate that hepatic deletion of *Prmt1*
433 may protect against pathological hepatic gluconeogenesis in type 1 diabetes.

434 In addition to type 1 diabetes, hepatic regulation of glucose constitutes a very important aspect
435 of liver dysfunction in various metabolic disorders. Chronic HFD feeding promotes obesity and
436 insulin resistance and has been used as a model to induce both type 2 diabetes and nonalcoholic
437 fatty liver disease (NAFLD) in mice (34). Mice on HFD had higher body weights and elevated
438 fasting blood glucose levels compared with mice on chow diet as expected (Figure 5F). qPCR
439 analyses showed that *Prmt1* was significantly induced in the liver by HFD feeding, accompanied
440 by the activation of gluconeogenic genes, including *Pck1*, *G6pc*, and *Cebpb* (Figure 5, G and H).
441 In particular, *Prmt1v2* was significantly increased in the liver from mice on HFD while there was
442 no difference in the expression of *Prmt1v1* between mice on chow diet and HFD (Figure 5G).

443 Similar to what was observed in STZ-induced type 1 diabetes model, when challenged with
444 HFD feeding, hepatic deletion of *Prmt1* provided protection against hyperglycemia in this type 2
445 diabetes model. Upon HFD feeding, *Alb-Cre;Prmt1^{fl/fl}* mice showed lower body weight gain and
446 less liver tissue mass than those of the littermate control animals without differences in food intake
447 (Figure 5, I and J, Supplementary Figure 7A). After fasting, blood glucose was lower and
448 gluconeogenic genes were less induced in the liver in *Alb-Cre;Prmt1^{fl/fl}* than those of controls
449 (Figure 5, K and L). *Alb-Cre;Prmt1^{fl/fl}* mice on HFD showed less impaired glucose tolerance
450 compared to littermate control while these two genotypes showed comparable glycemia control on
451 chow diet (Figure 5M, Supplementary Figure 7B). Together, these data indicate that inhibiting

452 hepatic PRMT1 activity may protect against inappropriate glucose production due to insulin
453 resistance.

454 In comparison to standard HFD, so called western diets, which contains high-fat, high
455 fructose and high cholesterol, are more widely used as a more specific model for fatty liver study,
456 which better mimics fast food style diets (34). It is of great interest to observe that *Prmt1*,
457 particularly *Prmt1v2* was increased in the livers of mice challenged with western diet and loss of
458 hepatic *Prmt1* protected mice from metabolic dysfunction caused by a western diet
459 (Supplementary Figure 8). These data indicate that PRMT1 may be involved in hepatic regulation
460 in a broad spectrum of metabolic disorders.

461

462

463

464

465

466

467

468

469

470

471

472

473

474

475

476

477

478

479

480 Discussion

481 Our study revealed that *Prmt1* deficiency results in impaired gluconeogenesis in the liver
482 during fasting. PRMT1V2 is the isoform that is primarily responsible for glucose regulation
483 through interactions with PGC1 α and this mechanism is conserved in human hepatocytes. Hepatic
484 deletion of *Prmt1* protects against inappropriate activation of gluconeogenesis in metabolic
485 disorder, such as diabetes.

486 The expression profiling of different isoforms of *Prmt1* showed that *Prmt1v2* was expressed
487 at a higher level than *Prmt1v1* in mouse and human hepatocytes. Functional analyses revealed that
488 PRMT1V2 activated the gluconeogenic program in the hepatocytes and augmented glucose
489 production in vivo, while there were no effects of PRMT1V1. The difference between *Prmt1v1*
490 and *Prmt1v2* is that there is a nuclear export sequence in *Prmt1v1* which makes PRMT1V1
491 exported to the cytoplasm and PRMT1V2 exist in the nucleus (16) (Figure 2, A and C), indicating
492 that PRMT1V2 may activate gluconeogenesis through modulating transcription, likely through
493 controlling methylation of transcriptional regulators, such as PGC1 α (Figure 3C, Figure 4, A-H).

494 A previous study has implicated that PRMT1 may be involved in glucose control through a
495 FOXO1-dependent mechanism (27). However, the differential regulation via different isoforms of
496 PRMT1 was not investigated. It is also of note that the levels of PRMT1 protein were significantly
497 reduced in the *Prmt1*^{+/-} mice in this previous study (27), whereas similar protein levels of PRMT1
498 were detected in the liver of *Alb-Cre;Prmt1*^{fl/+} mice compared to that in the control *Prmt1*^{fl/fl} mice
499 in our study. It is conceivable that systemic haploinsufficiency of PRMT1 may lead to secondary
500 influence on liver function and complicate the interpretation of the phenotype observed in *Prmt1*^{+/-}
501 mice. We observed that, when co-overexpressed, both PRMT1V1 and PRMT1V2 works with
502 FOXO1 to activates *Pck1* promoter activity regardless the presence or absence of PGC1 α ,
503 indicating that PRMT1 closely interacts with key modulators of liver glucose control through
504 multiple mechanisms.

505 Our study revealed a feedback regulation between PRMT1V2 and PGC1 α in hepatocytes.
506 PGC1 α was strongly induced in the liver of mice in the fasted state and overexpression of PGC1 α
507 through adenoviral delivery stimulated hepatic gluconeogenesis (4). Deletion of *Ppargc1a* reduced
508 the hepatic glucose production in the fasted mice (29). It has been reported that PGC1 α is induced
509 in STZ-induced and *db/db* diabetic mice (4, 35). Knockdown of *Ppargc1a* could reduce hepatic
510 gluconeogenesis in the diabetes mouse model (35). Intriguingly, it is also well documented that
511 *PPARGC1A* expression is reduced in the liver of humans with diabetes and NAFLD (36-38). The
512 precise modulation of PGC1 α activity in the liver is critical in systemic glucose control (39). Our
513 study suggests that PRMT1V2 represents another key module in this complex network that acutely
514 senses nutritional and hormonal cues and consists of many regulators, including PGC1 α and
515 FOXO1.

516 Protein arginine methylation is an important posttranscriptional modification for protein
517 function (40). It has been reported that multiple cellular processes are regulated by arginine
518 methylation, including RNA processing, signaling transduction, and transcriptional regulation (40).
519 PRMT1 is the key member of the PRMT family, which is responsible for most of the asymmetric
520 dimethylation. PRMT1 is expressed in various tissues (25). It has been reported that PRMT1 is
521 involved in a variety of biological processes, including transcriptional control, DNA repair, mRNA
522 splicing, and signal transduction (10). PRMT1 was further shown to play a role in cancer
523 progression (41) and thermogenesis activation in fat (15). Previous studies indicated that PRMT1
524 regulates lipogenesis in hepatic steatosis and alcohol-induced liver dysfunction (14, 26, 42-44).
525 Despite of the fact that pleiotropic effects of PRMT1 have been investigated in various tissues, the
526 unique discovery of the current study lies in the specific and finetuned regulation mediated by this
527 interaction between PGC1 α and PRMT1V2. This isoform specific coactivation is regulated
528 primarily by nucleus localized PRMT1V2. On the one hand, methylation-resistant form of PGC1 α
529 can still regulate gluconeogenesis (Figure 4, E and G), suggesting, not surprisingly, this master
530 regulator of liver function can be modulated by other factors besides PRMT1. Yet, the synergistic
531 effects between PGC1 α and PRMT1V2 are almost completely absent when arginine methylation
532 is blocked. Either loss of catalytical ability of PRMT1V2 or mutations in the potential arginine
533 methylation sites in PGC1 α abolished the synergistic effects of this PGC1 α and PRMT1 interaction.
534 PGC1 α is mechanistically involved in the glucagon mediated stabilization of PRMT1V2 on the
535 protein level, whereas, the other hormone crucial in glycemic control, insulin, posts minimal

536 effects in this process. The specificity at each step of this pathway may prove to be advantageous
537 when aiming for targeted effects in future efforts strategizing therapeutic intervention against
538 pathological hyperglycemia.

539 Lastly, our study revealed impressive functional significance of this interaction. With deletion
540 of *Prmt1* in hepatocytes, mice displayed better glycemia control and overall improved metabolic
541 health when challenged with STZ injection or HFD feeding, indicating that PRMT1 played a
542 critical role in the regulation of inappropriate hepatic glucose production in diabetes. Given that
543 *PRMTIV2* was significantly induced in the liver of multiple metabolic disease settings where liver
544 dysfunction is involved, ongoing drug development efforts to identify specific inhibitor for
545 PRMT1 may be of great therapeutic potential in the near future (45).

546

547

548

549

550 **Acknowledgements**

551 This work was supported by a grant from the American Diabetes Association (1-18-IBS-281
552 to JWu) and AGA-Allergan Foundation pilot research award from the American
553 Gastroenterological Association (AGA2020-21-09 to JWu), and fellowships from the Chinese
554 Scholarship Council (201806370290 to YM, 201908420207 to JWang). We thank Dr. Michael
555 Stallcup at the University of Southern California for sharing plasmids expressing PGC1 α - Δ E and
556 PGC1 α -R3K.

557

558 **Author contributions**

559 YM and JWu conceived the project and designed the study. YM, SL, HJ, JWang, XF, GL, JG
560 performed the experiments and analyzed the data. LY, LR and SAW provided reagents and
561 discussions. YM and JWu wrote the manuscript. JWu oversaw the study.

562

563 **Declaration of competing interest**

564 The authors declare no competing interests.

565 **References**

- 566 1. Rines, A. K., Sharabi, K., Tavares, C. D., and Puigserver, P. (2016) Targeting hepatic
567 glucose metabolism in the treatment of type 2 diabetes. *Nat Rev Drug Discov* **15**, 786-
568 804
- 569 2. Rui, L. (2014) Energy metabolism in the liver. *Compr Physiol* **4**, 177-197
- 570 3. Puigserver, P., Wu, Z., Park, C. W., Graves, R., Wright, M., and Spiegelman, B. M.
571 (1998) A cold-inducible coactivator of nuclear receptors linked to adaptive
572 thermogenesis. *Cell* **92**, 829-839
- 573 4. Yoon, J. C., Puigserver, P., Chen, G., Donovan, J., Wu, Z., Rhee, J., Adelmant, G.,
574 Stafford, J., Kahn, C. R., Granner, D. K., Newgard, C. B., and Spiegelman, B. M. (2001)
575 Control of hepatic gluconeogenesis through the transcriptional coactivator PGC-1.
576 *Nature* **413**, 131-138
- 577 5. Rhee, J., Inoue, Y., Yoon, J. C., Puigserver, P., Fan, M., Gonzalez, F. J., and
578 Spiegelman, B. M. (2003) Regulation of hepatic fasting response by PPARgamma
579 coactivator-1alpha (PGC-1): requirement for hepatocyte nuclear factor 4alpha in
580 gluconeogenesis. *Proc Natl Acad Sci U S A* **100**, 4012-4017
- 581 6. Rodgers, J. T., Lerin, C., Haas, W., Gygi, S. P., Spiegelman, B. M., and Puigserver, P.
582 (2005) Nutrient control of glucose homeostasis through a complex of PGC-1alpha and
583 SIRT1. *Nature* **434**, 113-118
- 584 7. Puigserver, P., Rhee, J., Donovan, J., Walkey, C. J., Yoon, J. C., Oriente, F., Kitamura,
585 Y., Altomonte, J., Dong, H., Accili, D., and Spiegelman, B. M. (2003) Insulin-regulated
586 hepatic gluconeogenesis through FOXO1-PGC-1alpha interaction. *Nature* **423**, 550-555
- 587 8. Lin, J., Handschin, C., and Spiegelman, B. M. (2005) Metabolic control through the
588 PGC-1 family of transcription coactivators. *Cell Metab* **1**, 361-370
- 589 9. Teyssier, C., Ma, H., Emter, R., Kralli, A., and Stallcup, M. R. (2005) Activation of
590 nuclear receptor coactivator PGC-1alpha by arginine methylation. *Genes Dev* **19**, 1466-
591 1473
- 592 10. Bedford, M. T., and Clarke, S. G. (2009) Protein arginine methylation in mammals: who,
593 what, and why. *Mol Cell* **33**, 1-13

- 594 11. Blanc, R. S., and Richard, S. (2017) Arginine Methylation: The Coming of Age. *Mol Cell*
595 **65**, 8-24
- 596 12. Iwasaki, H., and Yada, T. (2007) Protein arginine methylation regulates insulin signaling
597 in L6 skeletal muscle cells. *Biochem Biophys Res Commun* **364**, 1015-1021
- 598 13. Pyun, J. H., Kim, H. J., Jeong, M. H., Ahn, B. Y., Vuong, T. A., Lee, D. I., Choi, S., Koo,
599 S. H., Cho, H., and Kang, J. S. (2018) Cardiac specific PRMT1 ablation causes heart
600 failure through CaMKII dysregulation. *Nat Commun* **9**, 5107
- 601 14. Park, M. J., Kim, D. I., Lim, S. K., Choi, J. H., Kim, J. C., Yoon, K. C., Lee, J. B., Lee, J.
602 H., Han, H. J., Choi, I. P., Kim, H. C., and Park, S. H. (2014) Thioredoxin-interacting
603 protein mediates hepatic lipogenesis and inflammation via PRMT1 and PGC-1alpha
604 regulation in vitro and in vivo. *J Hepatol* **61**, 1151-1157
- 605 15. Qiao, X., Kim, D. I., Jun, H., Ma, Y., Knights, A. J., Park, M. J., Zhu, K., Lipinski, J. H.,
606 Liao, J., Li, Y., Richard, S., Weinman, S. A., and Wu, J. (2019) Protein Arginine
607 Methyltransferase 1 Interacts With PGC1alpha and Modulates Thermogenic Fat
608 Activation. *Endocrinology* **160**, 2773-2786
- 609 16. Goulet, I., Gauvin, G., Boisvenue, S., and Cote, J. (2007) Alternative splicing yields
610 protein arginine methyltransferase 1 isoforms with distinct activity, substrate specificity,
611 and subcellular localization. *J Biol Chem* **282**, 33009-33021
- 612 17. Tikhanovich, I., Zhao, J., Olson, J., Adams, A., Taylor, R., Bridges, B., Marshall, L.,
613 Roberts, B., and Weinman, S. A. (2017) Protein arginine methyltransferase 1 modulates
614 innate immune responses through regulation of peroxisome proliferator-activated
615 receptor gamma-dependent macrophage differentiation. *J Biol Chem* **292**, 6882-6894
- 616 18. Wu, J., Ruas, J. L., Estall, J. L., Rasbach, K. A., Choi, J. H., Ye, L., Bostrom, P., Tyra, H.
617 M., Crawford, R. W., Campbell, K. P., Rutkowski, D. T., Kaufman, R. J., and
618 Spiegelman, B. M. (2011) The unfolded protein response mediates adaptation to
619 exercise in skeletal muscle through a PGC-1alpha/ATF6alpha complex. *Cell Metab* **13**,
620 160-169
- 621 19. Liu, X., Li, H., Liu, L., Lu, Y., Gao, Y., Geng, P., Li, X., Huang, B., Zhang, Y., and Lu, J.
622 (2016) Methylation of arginine by PRMT1 regulates Nrf2 transcriptional activity during
623 the antioxidative response. *Biochim Biophys Acta* **1863**, 2093-2103
- 624 20. Sakamaki, J., Daitoku, H., Ueno, K., Hagiwara, A., Yamagata, K., and Fukamizu, A.
625 (2011) Arginine methylation of BCL-2 antagonist of cell death (BAD) counteracts its
626 phosphorylation and inactivation by Akt. *Proc Natl Acad Sci U S A* **108**, 6085-6090

- 627 21. Tong, X., Zhang, D., Charney, N., Jin, E., VanDommelen, K., Stamper, K., Gupta, N.,
628 Saldate, J., and Yin, L. (2017) DDB1-Mediated CRY1 Degradation Promotes FOXO1-
629 Driven Gluconeogenesis in Liver. *Diabetes* **66**, 2571-2582
- 630 22. Lai, Y., Li, J., Li, X., and Zou, C. (2017) Lipopolysaccharide modulates p300 and Sirt1 to
631 promote PRMT1 stability via an SCF(Fbx17)-recognized acetyldegron. *J Cell Sci* **130**,
632 3578-3587
- 633 23. Qiu, K., Liang, W., Wang, S., Kong, T., Wang, X., Li, C., Wang, Z., and Wu, Y. (2020)
634 BACE2 degradation is mediated by both the proteasome and lysosome pathways. *BMC*
635 *Mol Cell Biol* **21**, 13
- 636 24. Hatting, M., Tavares, C. D. J., Sharabi, K., Rines, A. K., and Puigserver, P. (2018)
637 Insulin regulation of gluconeogenesis. *Ann N Y Acad Sci* **1411**, 21-35
- 638 25. Tang, J., Frankel, A., Cook, R. J., Kim, S., Paik, W. K., Williams, K. R., Clarke, S., and
639 Herschman, H. R. (2000) PRMT1 is the predominant type I protein arginine
640 methyltransferase in mammalian cells. *J Biol Chem* **275**, 7723-7730
- 641 26. Zhao, J., Adams, A., Weinman, S. A., and Tikhanovich, I. (2019) Hepatocyte PRMT1
642 protects from alcohol induced liver injury by modulating oxidative stress responses. *Sci*
643 *Rep* **9**, 9111
- 644 27. Choi, D., Oh, K. J., Han, H. S., Yoon, Y. S., Jung, C. Y., Kim, S. T., and Koo, S. H.
645 (2012) Protein arginine methyltransferase 1 regulates hepatic glucose production in a
646 FoxO1-dependent manner. *Hepatology* **56**, 1546-1556
- 647 28. Jackson, M. I., Cao, J., Zeng, H., Uthus, E., and Combs, G. F., Jr. (2012) S-
648 adenosylmethionine-dependent protein methylation is required for expression of
649 selenoprotein P and gluconeogenic enzymes in HepG2 human hepatocytes. *J Biol*
650 *Chem* **287**, 36455-36464
- 651 29. Lin, J., Wu, P. H., Tarr, P. T., Lindenberg, K. S., St-Pierre, J., Zhang, C. Y., Mootha, V.
652 K., Jager, S., Vianna, C. R., Reznick, R. M., Cui, L., Manieri, M., Donovan, M. X., Wu, Z.,
653 Cooper, M. P., Fan, M. C., Rohas, L. M., Zavacki, A. M., Cinti, S., Shulman, G. I., Lowell,
654 B. B., Krainc, D., and Spiegelman, B. M. (2004) Defects in adaptive energy metabolism
655 with CNS-linked hyperactivity in PGC-1alpha null mice. *Cell* **119**, 121-135
- 656 30. Matsumoto, M., Poci, A., Rossetti, L., Depinho, R. A., and Accili, D. (2007) Impaired
657 regulation of hepatic glucose production in mice lacking the forkhead transcription factor
658 Foxo1 in liver. *Cell Metab* **6**, 208-216
- 659 31. Priya, G., and Kalra, S. (2018) A Review of Insulin Resistance in Type 1 Diabetes: Is
660 There a Place for Adjunctive Metformin? *Diabetes Ther* **9**, 349-361

- 661 32. Gastaldelli, A., and Cusi, K. (2019) From NASH to diabetes and from diabetes to NASH:
662 Mechanisms and treatment options. *JHEP Rep* **1**, 312-328
- 663 33. Wu, J., and Yan, L. J. (2015) Streptozotocin-induced type 1 diabetes in rodents as a
664 model for studying mitochondrial mechanisms of diabetic beta cell glucotoxicity.
665 *Diabetes Metab Syndr Obes* **8**, 181-188
- 666 34. Van Herck, M. A., Vonghia, L., and Francque, S. M. (2017) Animal Models of
667 Nonalcoholic Fatty Liver Disease-A Starter's Guide. *Nutrients* **9**
- 668 35. Koo, S. H., Satoh, H., Herzig, S., Lee, C. H., Hedrick, S., Kulkarni, R., Evans, R. M.,
669 Olefsky, J., and Montminy, M. (2004) PGC-1 promotes insulin resistance in liver through
670 PPAR-alpha-dependent induction of TRB-3. *Nat Med* **10**, 530-534
- 671 36. Ahrens, M., Ammerpohl, O., von Schonfels, W., Kolarova, J., Bens, S., Itzel, T., Teufel,
672 A., Herrmann, A., Brosch, M., Hinrichsen, H., Erhart, W., Egberts, J., Sipos, B.,
673 Schreiber, S., Hasler, R., Stickel, F., Becker, T., Krawczak, M., Rocken, C., Siebert, R.,
674 Schafmayer, C., and Hampe, J. (2013) DNA methylation analysis in nonalcoholic fatty
675 liver disease suggests distinct disease-specific and remodeling signatures after bariatric
676 surgery. *Cell Metab* **18**, 296-302
- 677 37. Koliaki, C., Szendroedi, J., Kaul, K., Jelenik, T., Nowotny, P., Jankowiak, F., Herder, C.,
678 Carstensen, M., Krausch, M., Knoefel, W. T., Schlensak, M., and Roden, M. (2015)
679 Adaptation of hepatic mitochondrial function in humans with non-alcoholic fatty liver is
680 lost in steatohepatitis. *Cell Metab* **21**, 739-746
- 681 38. Westerbacka, J., Kolak, M., Kiviluoto, T., Arkkila, P., Siren, J., Hamsten, A., Fisher, R.
682 M., and Yki-Jarvinen, H. (2007) Genes involved in fatty acid partitioning and binding,
683 lipolysis, monocyte/macrophage recruitment, and inflammation are overexpressed in the
684 human fatty liver of insulin-resistant subjects. *Diabetes* **56**, 2759-2765
- 685 39. Besse-Patin, A., Jeromson, S., Levesque-Damphousse, P., Secco, B., Laplante, M., and
686 Estall, J. L. (2019) PGC1A regulates the IRS1:IRS2 ratio during fasting to influence
687 hepatic metabolism downstream of insulin. *Proc Natl Acad Sci U S A* **116**, 4285-4290
- 688 40. Bedford, M. T., and Richard, S. (2005) Arginine methylation an emerging regulator of
689 protein function. *Mol Cell* **18**, 263-272
- 690 41. Yang, Y., and Bedford, M. T. (2013) Protein arginine methyltransferases and cancer. *Nat*
691 *Rev Cancer* **13**, 37-50
- 692 42. Zhao, J., Adams, A., Roberts, B., O'Neil, M., Vittal, A., Schmitt, T., Kumer, S., Cox, J., Li,
693 Z., Weinman, S. A., and Tikhanovich, I. (2018) Protein arginine methyl transferase 1-
694 and Jumonji C domain-containing protein 6-dependent arginine methylation regulate

- 695 hepatocyte nuclear factor 4 alpha expression and hepatocyte proliferation in mice.
696 *Hepatology* **67**, 1109-1126
- 697 43. Zhang, X. P., Jiang, Y. B., Zhong, C. Q., Ma, N., Zhang, E. B., Zhang, F., Li, J. J., Deng,
698 Y. Z., Wang, K., Xie, D., and Cheng, S. Q. (2018) PRMT1 Promoted HCC Growth and
699 Metastasis In Vitro and In Vivo via Activating the STAT3 Signalling Pathway. *Cell Physiol*
700 *Biochem* **47**, 1643-1654
- 701 44. Zhao, J., O'Neil, M., Vittal, A., Weinman, S. A., and Tikhanovich, I. (2019) PRMT1-
702 Dependent Macrophage IL-6 Production Is Required for Alcohol-Induced HCC
703 Progression. *Gene Expr* **19**, 137-150
- 704 45. Sun, Y., Wang, Z., Yang, H., Zhu, X., Wu, H., Ma, L., Xu, F., Hong, W., and Wang, H.
705 (2019) The Development of Tetrazole Derivatives as Protein Arginine Methyltransferase
706 I (PRMT1) Inhibitors. *Int J Mol Sci* **20**

707 **Figure legends**

708 **Figure 1.** Loss of *Prmt1* reduces gluconeogenic capacity in the liver. *A*) Body weights (left; n = 7
709 for ad lib, n = 6 for fasted), blood glucose levels (middle; n = 7/group), and qPCR analyses (right;
710 n = 7/group) of *Prmt1* and gluconeogenic marker mRNA levels in the liver of wild-type (WT)
711 mice under ad libitum-fed and 16 hour-fasted conditions. *B*) Immunoblot analyses of PRMT1 and
712 asymmetric-dimethylated arginine (Adme-R) in the liver of mice described in (*A*) (n = 3/group).
713 HSP90 was used as a loading control. *C*) Immunoblot (left) and quantification (right) analyses of
714 PRMT1 in the primary hepatocytes isolated from WT mice and treated with 100 µg/mL
715 cycloheximide (CHX) for indicated time after pretreatment with vehicle (Ctrl) or 200 nM glucagon
716 for 3 hours. α -tubulin was used as a loading control. *D*) Body weights of *Prmt1*^{fl/fl} and *Alb-*
717 *Cre;Prmt1*^{fl/fl} mice under basal conditions (chow diet, fed state, n = 6/group). *E*) H&E-stained
718 images of the liver in mice described in (*D*) (scale bar, 100 µm). *F*) qPCR analyses of *Prmt1*
719 mRNA levels across tissues from *Prmt1*^{fl/fl} and *Alb-Cre;Prmt1*^{fl/fl} mice (n = 4 for *Prmt1*^{fl/fl}, n = 3
720 for *Alb-Cre;Prmt1*^{fl/fl}). *G*) Immunoblot analyses of PRMT1 and Adme-R in the liver from mice
721 described in (*D*) (n = 2/group). HSP90 was used as a loading control. *H*) qPCR analyses of *Prmt1*
722 and gluconeogenic marker mRNA levels in *Prmt1*^{fl/fl} and *Alb-Cre;Prmt1*^{fl/fl} mice under basal
723 conditions (chow diet; fed state; n = 8 for *Prmt1*^{fl/fl}, n = 6 for *Alb-Cre;Prmt1*^{fl/fl}). *I*) Blood glucose
724 levels of 16 hour-fasted *Prmt1*^{fl/fl} and *Alb-Cre;Prmt1*^{fl/fl} mice (n = 6 for *Prmt1*^{fl/fl}, n = 5 for *Alb-*
725 *Cre;Prmt1*^{fl/fl}). *J*) qPCR analyses of *Prmt1* and gluconeogenic marker mRNA levels in the liver of

726 mice described in (I) (n = 4 for *Prmt1^{fl/fl}*, n = 6 for *Alb-Cre;Prmt1^{fl/fl}*). K) PTT in 16 hour-fasted
727 mice described in (I) (n = 6 for *Prmt1^{fl/fl}*, n = 5 for *Alb-Cre;Prmt1^{fl/fl}*). AUC, area under the curve.
728 L) qPCR analyses of *PRMT1* and *GFP* mRNA levels in HepG2 cells infected with indicated
729 adenoviruses (n = 6/group). M) qPCR analyses of gluconeogenic marker mRNA levels in HepG2
730 cells infected with indicated adenoviruses and stimulated with 1 mM glucagon plus 10 μ M
731 forskolin or vehicle (Ctrl) for 24 hours (n = 6/group). Data are presented as mean \pm SEM. **P* <
732 0.05; ***P* < 0.01; ****P* < 0.001. n.s., not significant. 2-tailed Student's *t* test (A, D, F, H-L) or 2-
733 way ANOVA (M).

734 **Figure 2.** PRMT1V2 (P1V2) is primarily responsible for the modulation of hepatic
735 gluconeogenesis. A) Schematic of *PRMT1V1* (*P1V1*) and *P1V2* transcript structure. B)
736 Immunoblot analyses of PRMT1 in purified nuclear and cytoplasmic fractions of liver from wild-
737 type (WT) mice under ad libitum-fed and 16 hour-fasted conditions. Histone H3 (H3) and α -tubulin
738 served as nuclear and cytoplasmic markers, respectively. C) Immunoblot analyses of PRMT1 in
739 purified nuclear and cytoplasmic fractions of Hepa 1-6 cells infected with indicated adenoviruses.
740 Histone H3 (H3) and α -tubulin served as nuclear and cytoplasmic markers, respectively. D) qPCR
741 analyses of *P1V1* and gluconeogenic marker mRNA levels after infection with indicated
742 adenoviruses in primary hepatocytes isolated from WT mice (n = 4/group). E) Immunoblot
743 analyses of HA-P1V1 with anti-HA antibody in primary hepatocytes described in (D) (n = 2/group).
744 HSP90 was used as a loading control. F) qPCR analyses of *P1V2* and gluconeogenic marker
745 mRNA levels after infection with indicated adenoviruses in primary hepatocytes isolated from WT
746 mice (n = 4/group). G) Immunoblot analyses of HA-P1V2 with anti-HA antibody in primary
747 hepatocytes described in (F) (n = 2/group). HSP90 was used as a loading control. H) Schematic of
748 the experiment. *Prmt1^{fl/fl}* mice were injected with indicated adenovirus through tail vein for CRE-
749 mediated deletion. Seven days after first injection, the mice were injected with indicated
750 adenoviruses through tail vein for gain-of-function. I) qPCR analyses of *P1V1* and *P1V2* mRNA
751 levels in the liver of 16 hour-fasted mice described in (H) (n = 4 for Ad-GFP and Ad-P1V2, n = 3
752 for Ad-P1V1). J) Immunoblot analyses of PRMT1 in the liver from mice described in (H) (n =
753 2/group). HSP90 was used as a loading control. K) Blood glucose levels in 6 hour- or 16 hour-
754 fasted mice described in (H) (n = 4 for Ad-GFP and Ad-P1V2, n = 3 for Ad-P1V1). L) qPCR
755 analyses of gluconeogenic markers and *GFP* mRNA levels in 16 hour-fasted mice described in
756 (H) (n = 4 for Ad-GFP and Ad-P1V2, n = 3 for Ad-P1V1). M) PTT in 16 hour-fasted mice

757 described in (H) (n = 4 for Ad-GFP and Ad-P1V2, n = 3 for Ad-P1V1). AUC, area under the curve.
758 N) qPCR analyses of *P1V1* and gluconeogenic marker mRNA levels in HepG2 cells infected with
759 indicated adenoviruses (n = 4/group). O) Immunoblot analyses of HA-P1V1 with anti-HA
760 antibody in HepG2 cells described in (N) (n = 2/group). HSP90 was used as a loading control. P)
761 qPCR analyses of *P1V2* and gluconeogenic marker mRNA levels in HepG2 cells infected with
762 indicated adenoviruses (n = 4/group). Q) Immunoblot analyses of HA-P1V2 with anti-HA
763 antibody in HepG2 cells described in (P) (n = 2/group). HSP90 was used as a loading control. Data
764 are presented as mean \pm SEM. * $P < 0.05$; ** $P < 0.01$; *** $P < 0.001$. n.s., not significant. 2-tailed
765 Student's *t* test (D, F, N, P) or 1-way ANOVA (I, K-M).

766 **Figure 3.** PRMT1V2 activates hepatic gluconeogenesis through PGC1 α . A) qPCR analyses of
767 *Ppargc1a* and gluconeogenic marker mRNA levels in primary hepatocytes isolated from wild-type
768 (WT) mice and infected with indicated adenoviruses (n = 4/group). B) qPCR analyses of *Ppargc1a*,
769 *P1V1*, *P1V2*, and gluconeogenic marker mRNA levels in primary hepatocytes isolated from WT
770 mice and infected with indicated adenoviruses (n = 4/group). C) Analyses of asymmetric
771 dimethylation of PGC1 α . Hepa 1-6 cells were infected with indicated adenoviruses. Lysates were
772 immunoprecipitated with an anti-PGC1 α antibody. Both input and immunoprecipitates were
773 analyzed by immunoblotting as indicated. D, E) *Pck1* promoter activity in Hepa 1-6 cells
774 transiently transfected with indicated vectors (n = 4/group). F) qPCR analyses of *Ppargc1a* mRNA
775 levels in Hepa 1-6 cells infected with indicated adenoviruses (n = 6/group). G, H) *Pck1* promoter
776 activity in Hepa 1-6 cells infected with indicated adenoviruses and then transiently transfected
777 with indicated vectors (n = 6/group). I) *Alb-Cre;Prmt1^{fl/fl}* mice were first injected with the
778 adenovirus encoding an shRNA specific to *Ppargc1a* through tail vein. Three days after the first
779 injection, the mice were injected with indicated adenoviruses through tail vein for gain-of-function.
780 Blood glucose levels of these mice after 16 hour fasting (n = 3 for Ad-GFP, n = 4 for Ad-P1V1
781 and Ad-P1V2). J) qPCR analyses of *Ppargc1a*, *P1V1*, *P1V2*, and gluconeogenic marker mRNA
782 levels in the liver of 16 hour-fasted mice described in (I) (n = 3 for Ad-GFP, n = 4 for Ad-P1V1
783 and Ad-P1V2). K) PTT in 16 hour-fasted mice described in (I) (n = 3 for Ad-GFP, n = 4 for Ad-
784 P1V1 and Ad-P1V2). AUC, area under the curve. L) qPCR analyses of *PPARGC1A* and
785 gluconeogenic marker mRNA levels in HepG2 cells infected with indicated adenoviruses (n =
786 4/group). M) qPCR analyses of *PPARGC1A*, *P1V1*, *P1V2*, and gluconeogenic marker mRNA
787 levels in HepG2 cells infected with indicated adenoviruses (n = 4/group). N, O) *Pck1* promoter

788 activity in HepG2 cells transiently transfected with indicated vectors (n = 4/group). Data are
789 presented as mean ± SEM. **P* < 0.05; ***P* < 0.01; ****P* < 0.001. n.s., not significant. 2-tailed
790 Student's *t* test (A, D, F, L, N), 1-way ANOVA (B, E, I- K, M, O), or 2-way ANOVA (G, H).

791 **Figure 4.** PRMT1V2 activates PGC1 α by asymmetric dimethylation. *A*) Schematic of PRMT1V2-
792 G98R mutant. *B*) Analyses of asymmetric dimethylation of PGC1 α . Hepa 1-6 cells were
793 transiently transfected with indicated plasmids. Lysates were immunoprecipitated with an anti-
794 PGC1 α antibody. Both input and immunoprecipitates were analyzed by immunoblotting as
795 indicated. *C*) *Pck1* promoter activity in Hepa 1-6 cells transiently transfected with indicated
796 vectors (n = 4/group). *D*) Schematic of PGC1 α mutants. WT, wild-type; AD, activation domain;
797 RS, serine/arginine-rich region; RRM: RNA recognition motif. *E-H*) *Pck1* promoter activity in
798 Hepa 1-6 cells transiently transfected with indicated vectors (n = 4/group). *I*) qPCR analyses of
799 *PRMT1* mRNA levels in HepG2 cells infected with indicated adenoviruses (n = 4/group). *J*)
800 Immunoblot analyses of PRMT1 in HepG2 cells described in (*I*) (n = 3/group). HSP90 was used
801 as a loading control. *K*) qPCR analyses of *EP300* and *SIRT1* in HepG2 cells described in (*I*) (n =
802 4/group). *L*) Immunoblot (left) and quantification (right) analyses of PRMT1 in primary
803 hepatocytes isolated from wild-type mice after injection with indicated adenovirus and treated with
804 100 μ g/mL cycloheximide (CHX) for indicated time after pretreatment with vehicle (Ctrl) or 200
805 nM glucagon for 3 hours. α -tubulin was used as a loading control. Data are presented as mean ±
806 SEM. ****P* < 0.001. n.s., not significant. 2-tailed Student's *t* test (E, G, I, K) or 1-way ANOVA
807 (C, F, H).

808 **Figure 5.** Hepatocyte-specific *Prmt1* deletion ameliorates diabetic hyperglycemia. *A*) Blood
809 glucose levels (left) and qPCR analyses of *Prmt1* and gluconeogenic marker (middle) and two
810 different *Prmt1* variants mRNA levels (right) in the liver from wild-type (WT) mice
811 intraperitoneally injected with vehicle (Ctrl) or 100 mg/kg streptozocin (STZ) daily for one week
812 (n = 5 for Ctrl, n = 4 for STZ). *B*) Immunoblot analyses of PRMT1 in the liver of mice described
813 in (*A*) (n = 3/group). HSP90 was used as a loading control. *C*) Blood glucose levels of *Prmt1*^{fl/fl}
814 and *Alb-Cre;Prmt1*^{fl/fl} mice in the fed state after daily intraperitoneal injection with 100 mg/kg
815 STZ for one week (n = 5 for *Prmt1*^{fl/fl}, n = 4 for *Alb-Cre;Prmt1*^{fl/fl}). *D*) qPCR analyses of *Prmt1*
816 and gluconeogenic marker mRNA levels in the liver of mice in the fed state described in (*C*) (n =
817 5 for *Prmt1*^{fl/fl}, n = 4 for *Alb-Cre;Prmt1*^{fl/fl}). *E*) GTT in 16 hour-fasted mice described in (*C*) (n =

818 5 for *Prmt1*^{fl/fl}, n = 4 for *Alb-Cre;Prmt1*^{fl/fl}). AUC, area under the curve. *F*) Body weight (left) and
819 16 hour-fasted blood glucose levels (right) in WT mice on chow diet or high fat diet (HFD) for 12
820 weeks (n = 4 for Chow, n = 8 for HFD). *G*) qPCR analyses of *Prmt1* and gluconeogenic marker
821 (left) and two different *Prmt1* variants (right) mRNA levels in the liver from mice described in (*F*)
822 (n = 5 for Chow, n = 8 for HFD). *H*) Immunoblot analyses of PRMT1 in the liver of mice described
823 in (*F*) (n = 3/group). HSP90 was used as a loading control. *I*) Changes in body weights of *Prmt1*^{fl/fl}
824 and *Alb-Cre;Prmt1*^{fl/fl} mice upon HFD (n = 5 for *Prmt1*^{fl/fl}, n = 8 for *Alb-Cre;Prmt1*^{fl/fl}). *J*) Liver
825 weight of *Prmt1*^{fl/fl} and *Alb-Cre;Prmt1*^{fl/fl} mice after 8 weeks on HFD (n = 5 for *Prmt1*^{fl/fl}, n = 8
826 for *Alb-Cre;Prmt1*^{fl/fl}). *K*) Blood glucose levels in 6 hour-fasted mice described in (*J*) (n = 5 for
827 *Prmt1*^{fl/fl}, n = 8 for *Alb-Cre;Prmt1*^{fl/fl}). *L*) qPCR analyses of *Prmt1* and gluconeogenic marker
828 mRNA levels in the liver of 6 hour-fasted mice described in (*J*) (n = 4/group). *M*) GTT in 16 hour-
829 fasted mice described in (*J*) (n = 5 for *Prmt1*^{fl/fl}, n = 8 for *Alb-Cre;Prmt1*^{fl/fl}). AUC, area under the
830 curve. Data are presented as mean ± SEM. **P* < 0.05; ** *P* < 0.01; ****P* < 0.001. n.s., not
831 significant. 2-tailed Student's *t* test (A, C-G, I-M).

Figure 1

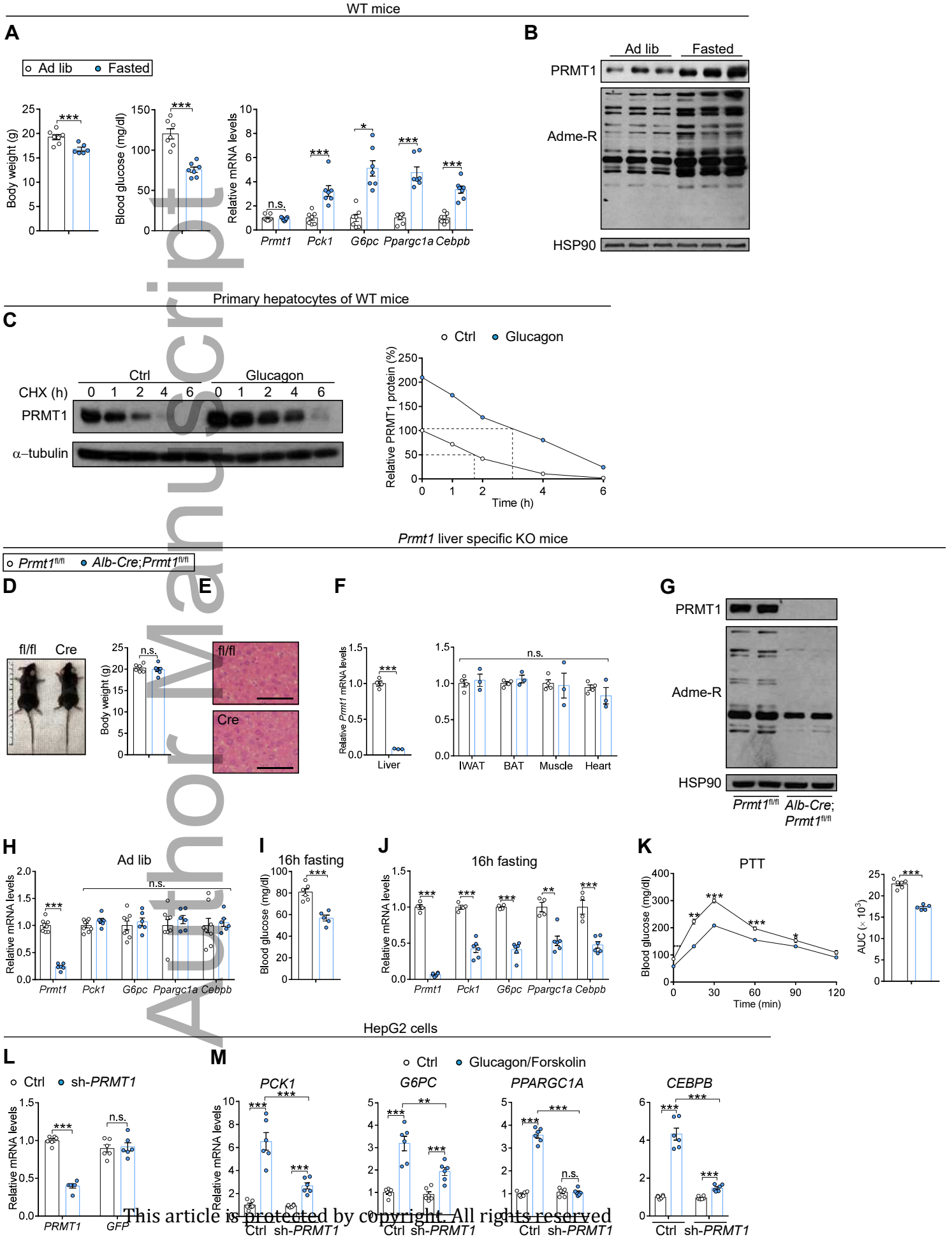


Figure 2

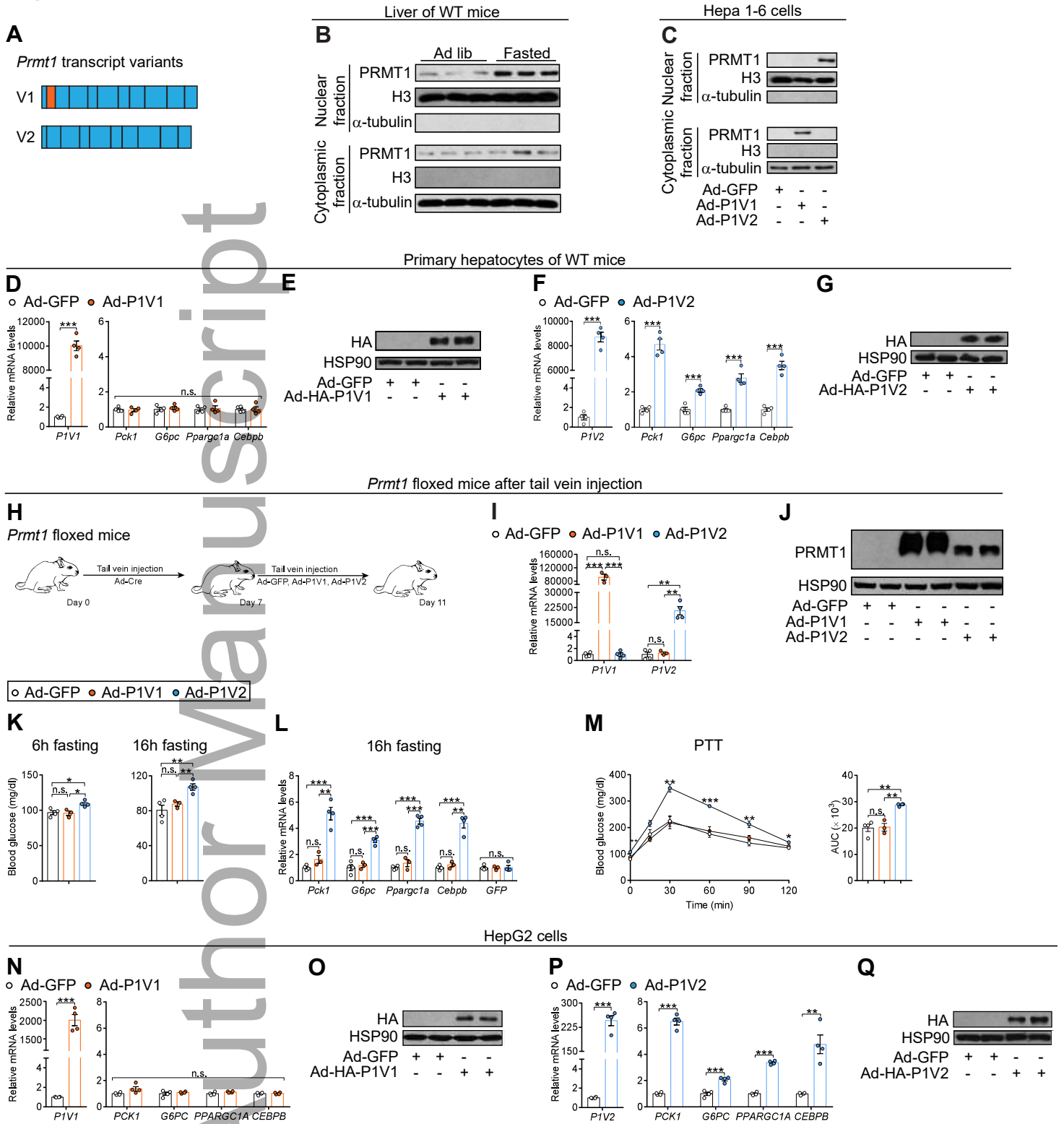


Figure 3

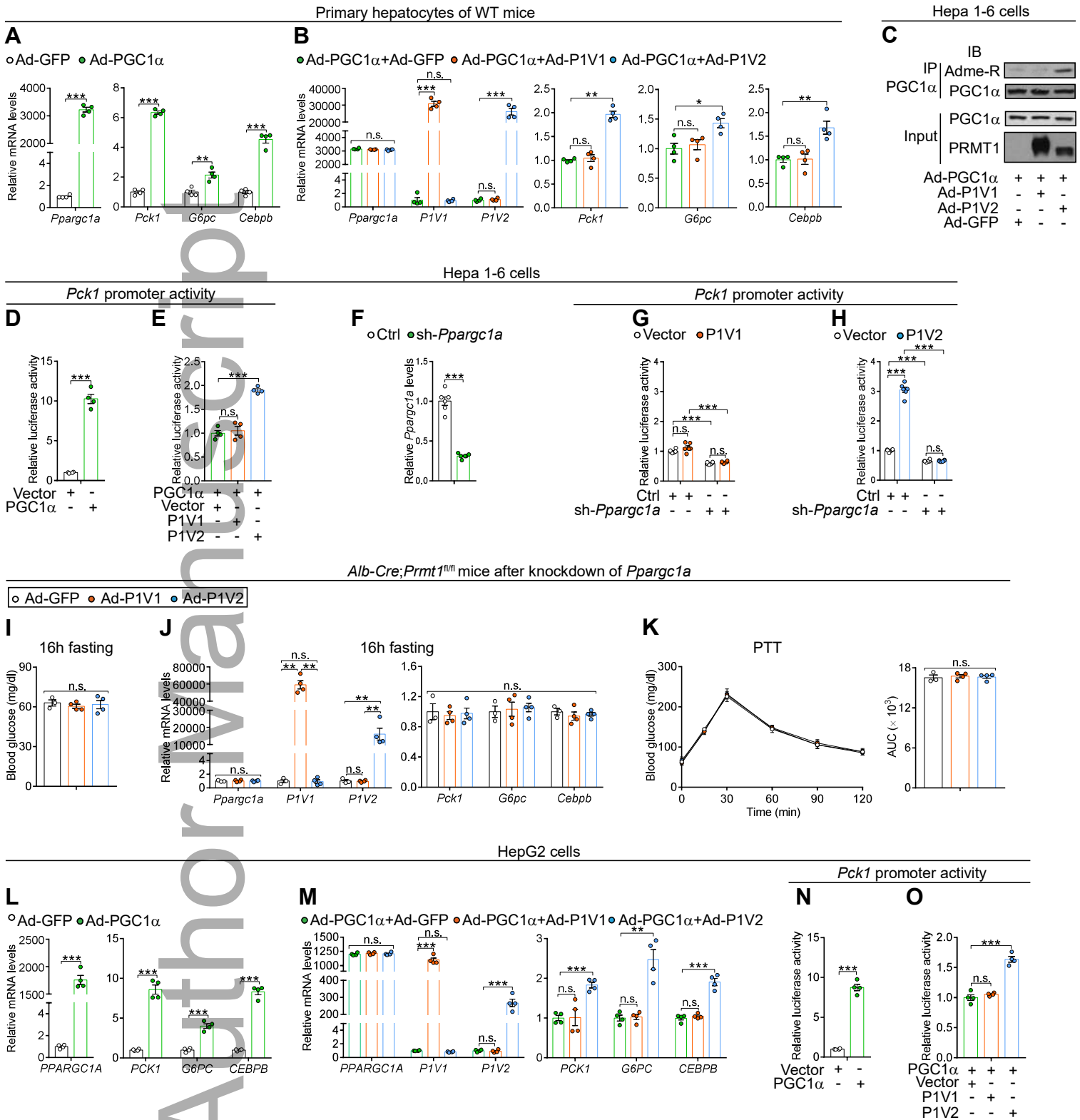


Figure 4

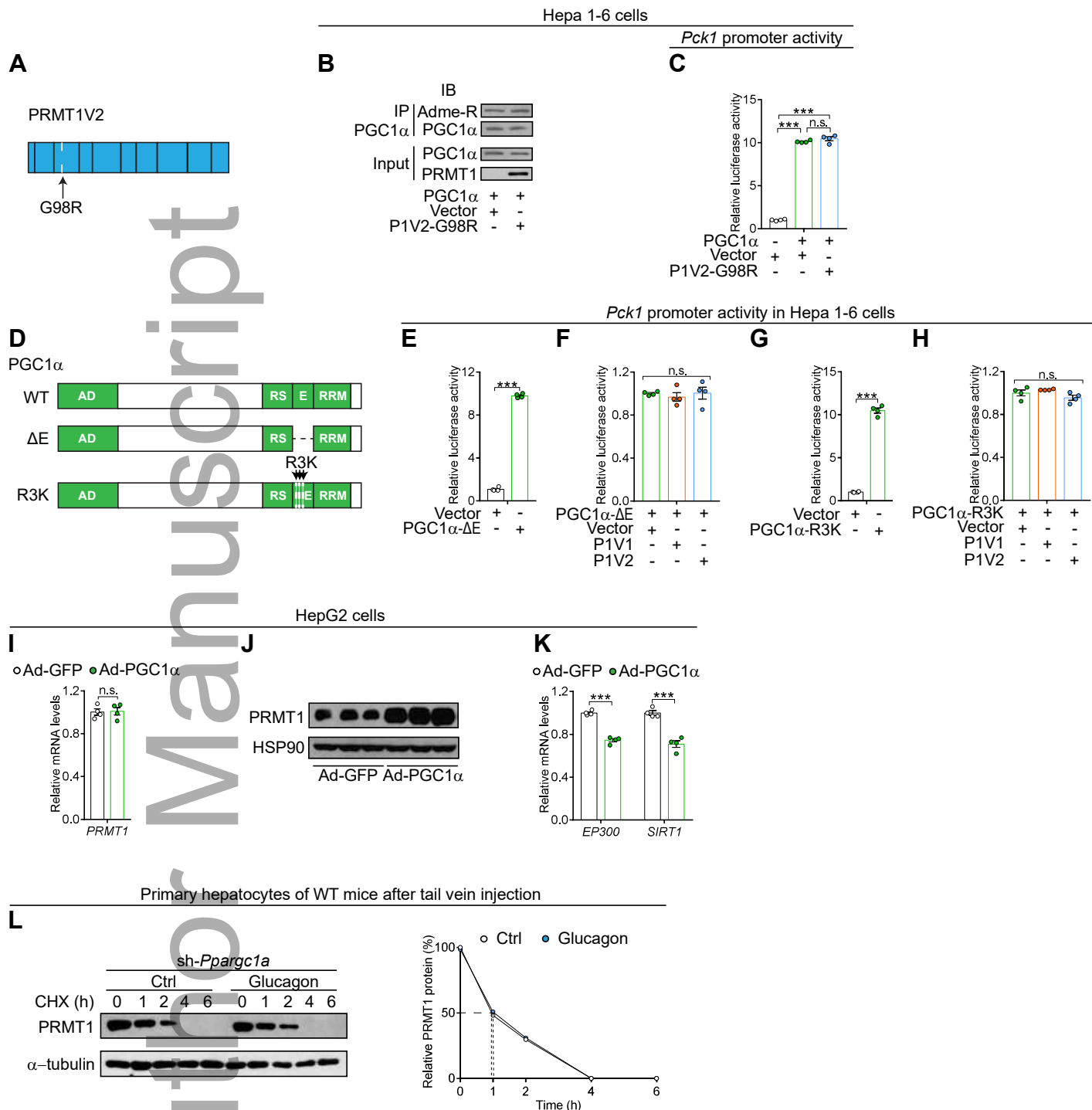


Figure 5

